

See discussions, stats, and author profiles for this publication at: <https://www.researchgate.net/publication/333188607>

Tropical Cyclone Activity over Bay of Bengal in relation to ENSO

Article in International Journal of Climatology · May 2019

DOI: 10.1002/joc.6165

CITATIONS
27

READS
681

3 authors:



Pankaj Bhardwaj

Government College Bahu (Haryana)

29 PUBLICATIONS 171 CITATIONS

[SEE PROFILE](#)



D. R. Pattanaik

India Meteorological Department

96 PUBLICATIONS 1,080 CITATIONS

[SEE PROFILE](#)



Omvir Singh

Kurukshetra University

98 PUBLICATIONS 1,019 CITATIONS

[SEE PROFILE](#)

Some of the authors of this publication are also working on these related projects:



groundwater dynamics and its economy in Haryana [View project](#)



Weather and Climate Services [View project](#)

Tropical cyclone activity over Bay of Bengal in relation to El Niño-Southern Oscillation

Pankaj Bhardwaj¹ | Dushmanta R. Pattanaik² | Omvir Singh¹ 

¹Department of Geography, Kurukshetra University, Kurukshetra, India

²India Meteorological Department, Mausam Bhawan, New Delhi, India

Correspondence

Omvir Singh, Department of Geography, Kurukshetra University, Kurukshetra 136119, India.
Email: ovshome@yahoo.com

Abstract

The present paper investigates the impact of El Niño-Southern Oscillation (ENSO) on the Bay of Bengal tropical cyclone (TC) activity and associated alterations in environmental conditions during post-monsoon (October–December) season for a period of 44 years (1972–2015). The analysis reveals that the post-monsoon season TCs frequency, accumulated cyclone energy (ACE) and power dissipation index (PDI) values are negatively correlated with the Niño 3.4 sea surface temperature (SST) anomalies (significant at the 95% confidence level). La Niña years are characterized by more frequent and intense cyclonic events compared with El Niño years. The mean ACE and PDI values are approximately two times higher in La Niña than El Niño years. The mean number of TC days per year is also higher in La Niña (7.64 days) than El Niño (3.68 days) years (significant at 95% confidence level). In addition, a significant shift in genesis locations, tracks and landfalling locations of TCs has been observed under different ENSO phases. The mean genesis location of TCs have shifted eastward with tendency of more recurring tracks in La Niña than El Niño years. The presence of strong convective activity, reduced vertical wind shear, high SST ($\geq 28^{\circ}\text{C}$), enhanced mid-tropospheric relative humidity and low-level cyclonic circulation aids the TCs formation and strengthening during La Niña and vice-versa in El Niño conditions.

KEY WORDS

Bay of Bengal, El Niño-Southern Oscillation, environmental conditions, post-monsoon season, tropical cyclones

1 | INTRODUCTION

Tropical cyclones (TCs) are one of the most devastating severe weather systems causing huge losses of property and life via accompanying strong winds, intense rainfall, high storm surges and coastal inundation (Peduzzi *et al.*, 2012). The formation of TCs primarily depends on the large-scale oceanic and atmospheric conditions. Gray (1968, 1975) identified the six dynamic and thermodynamic parameters (also known as Grey's parameters) favourable for the genesis of TCs: (a) high low-level relative vorticity, (b) coriolis

force, (c) weak vertical wind shear (VWS), (d) sea surface temperature (SST) $> 26^{\circ}\text{C}$, (e) conditional instability and (f) high relative humidity (RH) in the lower and middle troposphere. Although these conditions are not sufficient for cyclogenesis, however, TC formation will be higher in the regions and seasons when the product of the above discussed parameters is maximum (Gray, 1975). TCs most often occur during the late summer to early autumn period when SST is maximum (Gutzler *et al.*, 2013; Zhao and Raga, 2015). The TCs mainly forms in the seven tropical ocean basins namely North Atlantic Ocean, eastern and western parts of North

Pacific Ocean, southwestern Pacific, southwestern and southeastern Indian Ocean and North Indian Ocean region. The cyclonic storms are often known as hurricanes and typhoons in the Atlantic and northwest Pacific, whereas TCs in other Ocean basins.

El Niño-Southern Oscillation (ENSO) is well known mode of tropical coupled atmosphere-ocean system causing alterations in the atmospheric and oceanic conditions far beyond the basins of their evolution (Trenberth, 1997; McPhaden, 2002). The two extremes associated with ENSO, termed El Niño (abnormal warming) and La Niña (abnormal cooling) events, describe the SST anomalies (SSTAs) in the central Pacific Ocean (Bjerknes, 1969). The warming of eastern tropical Pacific typically reaches at its peak during the end of calendar year (Trenberth, 1997; Tziperman *et al.*, 1998). ENSO events occur in every 2–7 years and last approximately 12–18 months with large variation in strengths (Chang *et al.*, 2006). In recent years, many researchers have paid attention towards the association between ENSO phenomena and TC activity (e.g., number, genesis location, track and intensity). The mean lifetime, frequency and intensity of TCs tends to increase during strong El Niño events over western, central and eastern North Pacific (Chan, 1985; Chu and Wang, 1997; Clark and Chu, 2002; Wang and Chan, 2002; Camargo and Sobel, 2005; Chen *et al.*, 2006; Chen and Huang, 2006), while in Atlantic region these are more active during La Niña years (Gray, 1984). Wang and Zhou (2008) reported the more frequent rapid intensification (typically defined as intensification of 30 knots or greater in 24 hr) of events in El Niño (53% of TCs) than La Niña years (37% of TCs) in the northwest Pacific. Klotzbach (2012) demonstrated the enhanced Atlantic TC activity and nearly three times as many rapid intensification events during La Niña, than El Niño years. Besides, several researchers have examined the impact of ENSO on TCs activity for different ocean basins (Clark and Chu, 2002; Tang and Neelin, 2004; Camargo *et al.*, 2008; Kuleshov *et al.*, 2008; Klotzbach, 2011; Xu and Huang, 2015). This review indicates that a comprehensive literature is available on the influence of ENSO on TC activity in the Pacific and Atlantic Oceans.

The North Indian Ocean alone accounts approximately 7% of global TCs, with a frequency about four to five times higher in the Bay of Bengal (BoB) compared with that in the Arabian Sea (Neumann, 1993; Dube *et al.*, 1997). Moreover, BoB TCs are usually more intense than Arabian Sea and leads to huge losses of property and life via accompanying strong winds, intense rainfall, high storm surges and coastal inundation. For example, Orissa super cyclone of 1999 have caused about 10,000 deaths and cyclone Nargis of 2008 caused about 138,000 deaths in Myanmar (Chittibabu *et al.*, 2004; Fritz *et al.*, 2009). Furthermore, the BoB TCs exhibits

a unique bimodal pattern in their occurrence with first lower peak in the pre-monsoon season (March–May) and second highest peak in the post-monsoon season (October–December) (Li *et al.*, 2013). Similarly, ENSO has the property of seasonal progressions, with SSTAs start to rise during April–June, thereby attaining highest peak nearly in October–December months in the central Pacific Ocean (Tziperman *et al.*, 1998; Picaut *et al.*, 2001). Hence, alterations in the oceanic and atmospheric conditions during different ENSO phases affect the TC activity in BoB (Singh *et al.*, 2001). However, research on the impact of ENSO on TCs over the BoB is far less compared with other ocean basins (Girishkumar and Ravichandran, 2012; Ng and Chan, 2012; Felton *et al.*, 2013; Girishkumar *et al.*, 2015). Recently, researchers have focused on modelling to establish the relationship between ENSO and BoB TCs (Balaguru *et al.*, 2016; Anandh *et al.*, 2018; Biswas and Kundu, 2018). Apart from this, modulated BoB TC activity owing to ENSO can create catastrophic destruction after landfalling on account of low-lying topography and high population density along the coastline. Better understanding of BoB TC activity in relation to ENSO is scientifically and socially important to minimize their effects. Therefore, main objective of the present study is to examine the impacts of ENSO on BoB TC activity during the period 1972 to 2015. This study also seeks to investigate the ENSO induced modulations in oceanic and atmospheric conditions over BoB.

2 | DATA AND METHODOLOGY

The Joint Typhoon Warning Centre (JTWC) best track data has been utilized in this study for the BoB TCs for the period 1972–2015 (Chu *et al.*, 2002). Until 1971, satellite data were not used operationally to estimate intensity and centre location at the JTWC. From 1972, satellite detection of TCs for North Indian Ocean was started by JTWC (Singh, 2010). This is the only database which provides TCs data with intensity information since 1972 over North Indian Ocean (Klotzbach and Oliver, 2015). The dataset comprises information of TCs name, position (latitude and longitude), minimum surface central pressure, and 1-min maximum sustained wind (MSW) speed at 6-hr intervals (0000, 0600, 1200, and 1800 UTC). Data related to various atmospheric variables (i.e., winds at 850 and 200 hPa, RH at 500 hPa and 500-hPa geopotential height) have been obtained from the National Centers for Environmental Prediction-National Center for Atmospheric Research (NCEP-NCAR) monthly reanalysis dataset with a $2.5^\circ \times 2.5^\circ$ longitude/latitude resolution (Kalnay *et al.*, 1996). Monthly 500-hPa outgoing longwave radiation (OLR) data have been extracted from the National Oceanic and Atmospheric Administration (NOAA) interpolated OLR data set (Liebmann and Smith, 1996)

starting from 1974 with a spatial resolution of 2.5° , available at the website of the NOAA-Climate Diagnostic Center (CDC) (<http://www.cdc.noaa.gov/>). The NOAA extended reconstructed monthly SST version 4 data, also available from NOAA-CDC, with a horizontal resolution of $2.0^\circ \times 2.0^\circ$ latitude-longitude has been used (Huang *et al.*, 2015).

2.1 | Classification of cyclonic storms

India Meteorological Department has classified the low pressure systems over the North Indian Ocean on the basis of MSW speed at surface level as shown in Table 1. In this study, first three categories (when MSW is <34 knot) have been excluded and focused only on the TCs (when MSW is ≥ 34 knot). If a system is reached atleast once (one 6-hr period) at the intensity of 34 knot or above in entire lifetime is considered as a TC. To calculate the number of TC days, the total number of 6-hourly periods have been divided by four and summed for the season. If any TC of a season happens to cross years, that cyclone counts for the previous year.

2.2 | Tropical cyclone energy metrics

Two frequently used TC energy metrics that is, accumulated cyclone energy (ACE) (Bell *et al.*, 2000) and power dissipation index (PDI) (Emanuel, 2005) have been computed to characterize the overall TC activity over BoB. ACE can be defined as, $ACE = \sum V_{max}^2$ having units (10^4 kt^2), where

TABLE 1 IMD's classification of cyclonic disturbances in the North Indian Ocean since 2015 (Bay of Bengal and Arabian Sea)

Type	Wind speed in km/h	Wind speed in knot (mps)	Number of closed isobars at interval of 2 hPa within 5° latitude/longitude square
Low pressure area (L)	Less than 31	Less than 17 (09)	1
Depression (D)	31–49	17–27 (9–14)	2
Deep depression (DD)	50–61	28–33 (15–17)	3
CS	62–88	34–47 (18–24)	4–7
SCS	89–118	48–63 (25–32)	8–10
VSCS	119–165	64–89 (33–46)	11–25
ESCS	166–220	90–119 (47–61)	26–39
SupCS	221 or more	120 (62) or more	40 or more

Note: Generic names such as tropical cyclone or cyclone is used to represent CS, SCS, VSCS, ESCS and SupCS as a whole.

V_{max} is intensity (MSW) of TC. ACE is the sum of V_{max} squared at all 6-hourly periods when the TC is at least of tropical storm strength (≥ 34 knots). The annual ACE has been calculated by summing up the ACE of all TCs in a year. PDI, defined as $PDI = \sum V_{max}^3$ having units (10^6 kt^3), analogous to ACE, is a widely used parameter to characterize the destructive potential of TCs. PDI is approximately proportional to the amount of monetary damage or power dissipation generated by a TC. Both energy metrics take into account the collective effect of frequency, intensity and duration of all the TCs in the season. ACE accounts for both the strength and duration while PDI emphasized more on TC intensity.

2.3 | Classification of ENSO years

To identify the occurrence and classification of ENSO events, several methods and indices have been developed world over. Southern Oscillation Index, oceanic Niño 1 + 2, Niño 3, Niño 3.4 and Niño 4 SST are most commonly used indices to indicate the occurrence of ENSO events (Rasmusson and Carpenter, 1982; Trenberth, 1984, 1997). Oceanic Niño Index (ONI) based on Niño 3.4 region SSTAs (5°S – 5°N , 170°W – 120°W) has been used most commonly to identify the ENSO events (Camargo and Sobel, 2005). Therefore, ONI data based on the 30-year period 1981–2010 has been archived from the website of NOAA's Climatic Prediction Center (<http://www.cpc.ncep.noaa.gov/>) (Smith and Reynolds, 2003). To identify the possible relationship between Niño 3.4 SST and BoB TCs activity, the acquired ONI values have been averaged for different seasons, that is, winter (January–February), pre-monsoon (March–May), monsoon (June–September) and post-monsoon (October–December), and correlated with number of TC, ACE and PDI of the same seasons separately. Interestingly, the mean ONI values of only post-monsoon season are significantly correlated with the frequency of TCs (correlation coefficient (CC) value = -0.36), ACE (CC value = -0.37) and PDI (CC value = -0.33), significant at the 95% confidence level. Besides, SSTAs in the central Pacific Ocean reached at its peak during this season (Tziperman *et al.*, 1998). Therefore, mean ONI of post-monsoon season has been used to identify the ENSO years. El Niño (La Niña) years selected if mean ONI mounted above 0.5°C (dropped below -0.5°C). A total of 15 El Niño (warm regime; 1972, 1976, 1977, 1982, 1986, 1987, 1991, 1994, 1997, 2002, 2004, 2006, 2009, 2014 and 2015), 14 La Niña (cold regime; 1973, 1974, 1975, 1983, 1984, 1988, 1995, 1998, 1999, 2000, 2007, 2008, 2010 and 2011) and remaining 15 have been identified as Neutral years during the period 1972–2015. Warm and cold conditions prevailed for approximately 34 and 32% of time, respectively during 44 years.

For quantitative analysis of this data, simple numerical calculations such as sums, frequencies, percentages, averages and standard deviations (SDs) have been computed. Subsequently, derived statistics have been summarized in the form of tables and graphs. The student's *t* test has been performed to assess the significance of trends in the TCs characteristics and to identify the difference in the means between El Niño and La Niña years, at 95% of confidence level. In addition, Karl Pearson's method of correlation analysis has been computed.

3 | RESULTS AND DISCUSSION

3.1 | Climatology of Bay of Bengal tropical cyclones

Figure 1 exhibits the annual distribution of TC frequency, ACE and PDI in the BoB during 1972–2015. A total of 144 TCs have occurred at the rate of 3.27 cyclones per year, with a SD of 1.56. The time series of the annual frequency of TCs shows a notable fluctuation ranging from 0 (2001) to 7 (1987). The mean annual ACE and PDI value is 12.84 (SD = 9.42) and 9.35 (SD = 8.77), respectively. Similar to the TCs frequency, annual ACE and PDI exhibits the large fluctuations with lowest value in 2001 (0) and maximum in 2013 (44 and 38). However, no statistically significant upward and downward trend has been observed in these three parameters. Of the total 144, approximately 27, 21, 8 and 7% TCs have reached at the intensity of severe cyclonic storms (SCS), very severe cyclonic storm (VSCS), extremely severe cyclonic storm (ESCS) and super cyclonic storm (SupCS), respectively.

Monthly occurrence of TCs of different intensity and mean ACE and PDI has been highlighted in the Figure 2. A unique bimodal pattern has been observed in the occurrence of TCs, ACE and PDI over BoB. First lower peak has been witnessed in the month of May (0.5 TC/year) while second

highest peak in November (1 TC/year) month, when environmental conditions are most favourable for the genesis of TCs over the BoB. A dramatic increase in the mid-level atmospheric RH is largely responsible for the first peak season whereas second highest peak is attributed to the reduced VWS (Li *et al.*, 2013). During the active monsoon season, SST exceeds the threshold value (26.5°C) and most active convection occurs over BoB (Yanase *et al.*, 2012). However, the strong VWS inhibits the genesis of TCs during this season (Gray, 1968). Apart from this, decreased frequency of TCs after the second highest peak is attributed to the reduced RH and low-level vorticity. The occurrence of TCs has been found negligible in the months of February and August. Of the total 10 SupCS, eight occurred in the months of April and October (four each) and two occurred in May and November months (one each). In addition, approximately 64% events (92 TCs) occurred during the post-monsoon season (hereafter referred as peak TC season). Annual TCs has strong correlation with peak season TCs frequency (CC value = 0.75, significant at the 99% confidence level). Hence, the subsequent sections of this paper will emphasize on the peak TC season over BoB. The main focus towards the peak TC season can be owed to following four reasons: (a) the peak season accounts approximately 64% of total TC number, (b) about 63% of total VSCS ($MSW \geq 64$ knot) noted in this season, (c) the peak season TCs significantly correlated with the annual TCs frequency and (d) mean Niño 3.4 SSTAs of post-monsoon season are significantly correlated with occurrence of TCs, ACE and PDI of the peak season.

3.2 | Impact of ENSO on peak season TC activity

Figure 3 exhibits the time series of number of TCs, ACE and PDI for the peak TCs season during the period 1972–2015. The mean number of TCs, ACE and PDI during

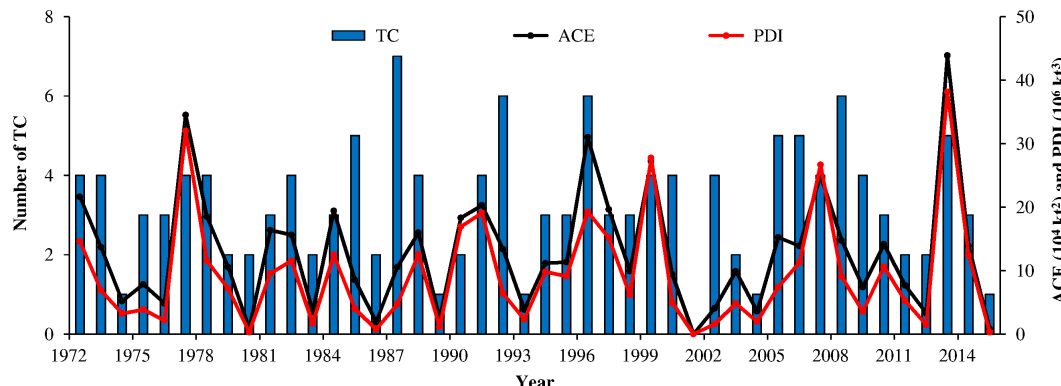


FIGURE 1 Bars showing the interannual variability in TCs over BoB during the period 1972–2015. The overlaid black and red solid lines with dots represent the ACE and PDI values, respectively [Colour figure can be viewed at wileyonlinelibrary.com]

FIGURE 2 Bars showing the monthly TC numbers of different intensity over BoB during 1972–2015. The overlaid black and red curves with dots represent the monthly mean ACE and PDI values, respectively. The values above each bar represent the TC numbers per year in that month [Colour figure can be viewed at wileyonlinelibrary.com]

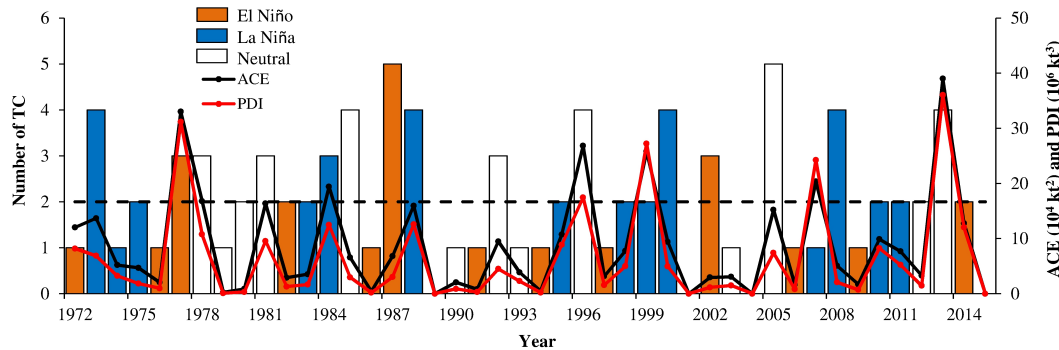
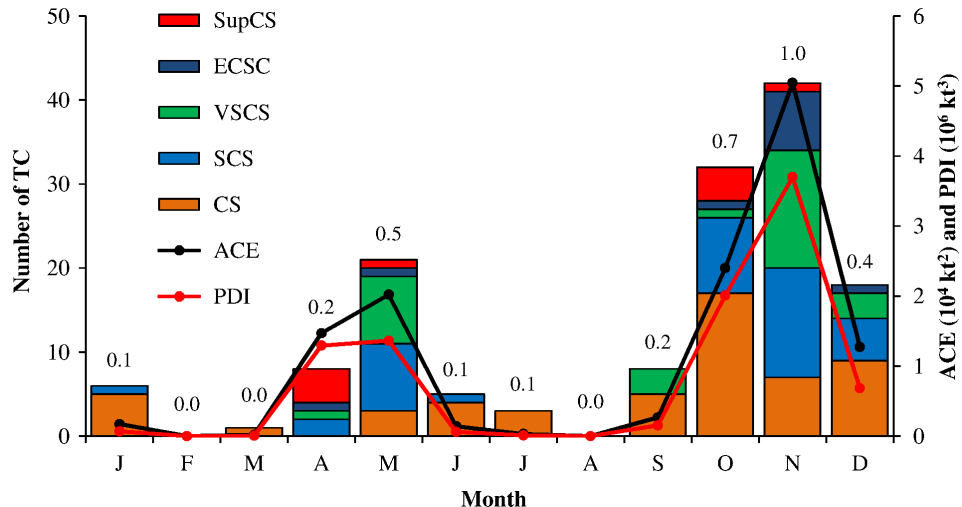


FIGURE 3 Bars showing the interannual variability in post-monsoon TCs over BoB during different ENSO years (1972–2015). Black dashed horizontal line shows the mean number of TCs. The overlaid black and red solid lines with dots represent the ACE and PDI values, respectively, for the post-monsoon season [Colour figure can be viewed at wileyonlinelibrary.com]

the post-monsoon season is 2.09 (SD = 1.38), 8.72 (SD = 9.33) and 6.39 (SD = 8.68), respectively. Of the total 92 TCs that formed during the peak season, 35 (38%) formed in La Niña while 23 (25%) formed in El Niño years. The computed mean number of TCs per year during El Niño, La Niña and neutral years are 1.53 (SD = 1.30), 2.50 (SD = 1.09) and 2.27 (SD = 1.58), respectively. The difference in mean number of TCs in El Niño and La Niña years is statistically insignificant as their difference is just 1.0 (Table 2). The computed mean ACE values per year during El Niño, La Niña and neutral years are 5.39 (SD = 8.65), 11.37 (SD = 6.78) and 9.57 (SD = 11.40), whereas mean PDI values per year are 4.11 (SD = 8.23), 8.89 (SD = 7.98) and 6.34 (SD = 9.64), respectively. The value of ACE and PDI during La Niña years is almost double of El Niño years, which is statistically significant at 95% confidence level. Similarly, the frequency of intense cyclones (VSCS, ESCS, SupCS) is higher in the La Niña years than El Niño (Table 2). These results are consistent with earlier studies (Mahala *et al.*, 2015; Mohapatra and Kumar, 2016). It has

been reported that during La Niña (El Niño) years, mean genesis location of TCs in northwest Pacific shifts westward (eastward) and have a tendency to follow westward (tend to curve northeastward) track (Chan, 1985, 2000; Lander, 1994; Wang and Chan, 2002). The reasonable cause for the greater frequency of TCs in La Niña years over BoB may be a result of redevelopment of the remnants of TCs of northwest Pacific.

In addition, Table 3 exhibits that out of total 15 El Niño years, 12 years (80% of the total) have normal or below normal (BN) TCs frequency while 3 years (20% of the total) have above normal (AN) frequency. Conversely, out of total 14 La Niña years, 12 years (86% of the total) has normal or above normal TCs frequency while only 2 years (14% of the total) have below normal frequency. The mean frequency of TCs is very high in the above normal TCs frequency years under El Niño conditions (3.67) than mean of 44-years post-monsoon period (2.09) and mean of El Niño years (1.53). Out of total 11 TCs occurred in these 3 years, three are SCS (MSW 48–63 knot) and two are ESCS (MSW \geq 90 knot)

TABLE 2 Number of TCs of different intensity, ACE and PDI during ENSO years (1972–2015)

	No. of years	CS	SCS	VSCS	ECSC	SupCS	Total	Av. per year
El Niño	15	10 (9.66) (3.73)	9 (14.62) (6.99)	0 (0.00) (0.00)	4 (56.51) (50.92)	0 (0.00) (0.00)	23 (80.79) (61.63)	1.53 (5.39) (4.11)
La Niña	14	11 (10.64) (3.96)	9 (24.15) (11.86)	8 (41.92) (26.21)	3 (29.46) (24.21)	4 (53.01) (58.24)	35 (159.17) (124.48)	2.50 (11.37) (8.89)
Neutral	15	12 (15.49) (6.22)	9 (30.36) (15.28)	10 (61.90) (36.55)	2 (16.08) (13.00)	1 (19.80) (24.07)	34 (143.62) (95.12)	2.27 (9.57) (6.34)
Total	44	33 (35.78) (13.91)	27 (69.13) (34.13)	18 (103.81) (62.76)	9 (102.05) (88.12)	5 (72.81) (82.31)	92 (383.58) (281.24)	2.09 (8.72) (6.39)

Note: Figures within the parentheses are ACE and PDI (Boldface) values.

which can cause immense damage of infrastructure and human casualties. Similarly, in the five above normal frequency years of La Niña conditions, the mean frequency of TCs is 3.80, which is very high than 2.09 (mean of 44-years post-monsoon period) and 2.50 (mean of La Niña years).

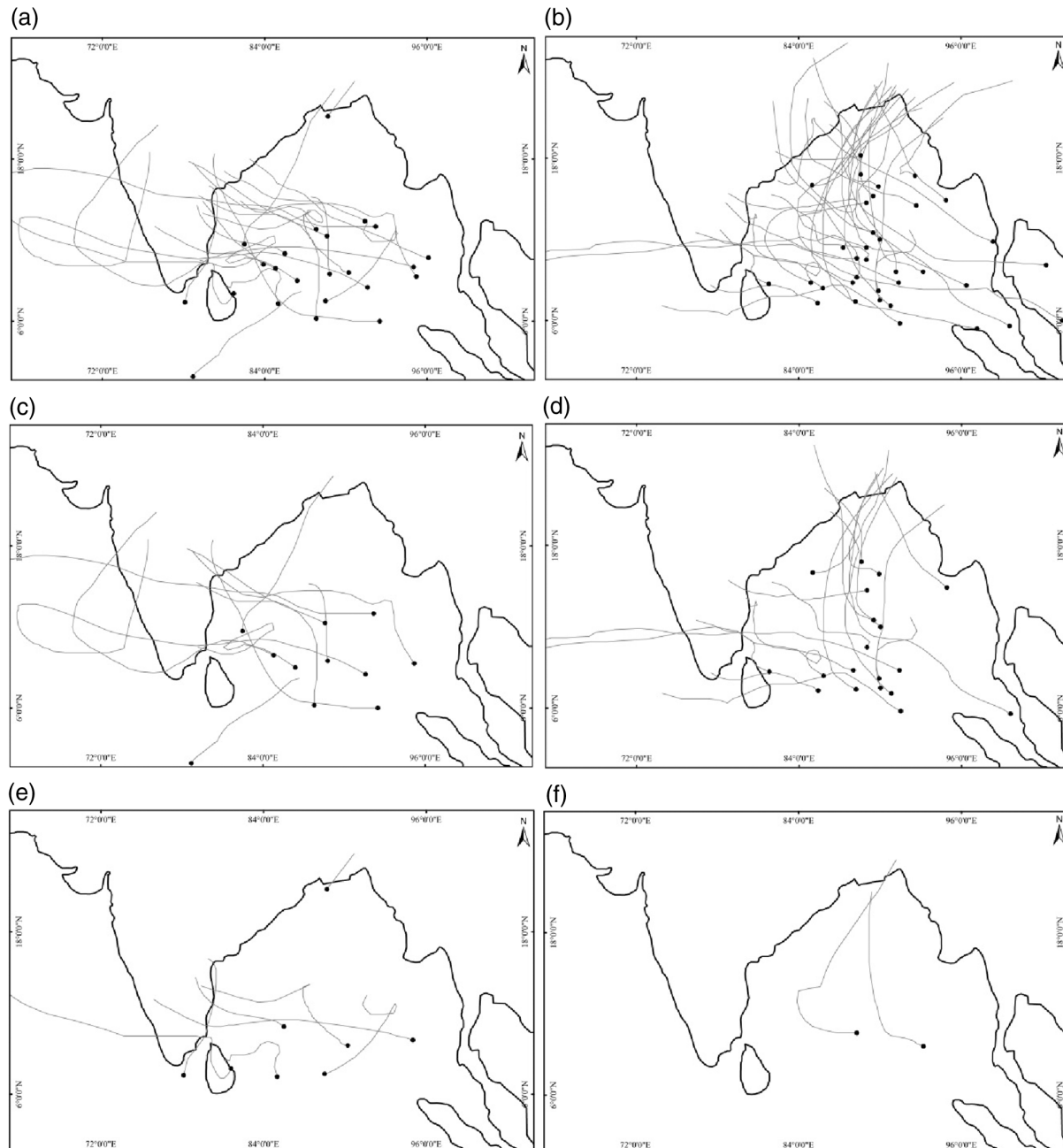
Large spatial variations are evident in the genesis locations, tracks and landfall patterns of TCs under different ENSO phases (Figure 4). Although majority of the peak season TCs formation is concentrated between 5° and 16°N latitudes; however, a longitudinal shift can be seen clearly in their genesis location. Approximately two-third of the total TCs during La Niña (El Niño) years formed eastward (westward) side of 89°E longitude (Figure 4a,b). During La Niña years, the mean genesis location of TCs is 90°93'E, 10°68'N, while in El Niño years it is 87°88'E, 9°86'N. The difference in the mean genesis location of TCs is about 3° longitude during different ENSO years. The TCs of La Niña years have to travel long distances and reach at mature stage prior to landfall and vice versa in El Niño years. The lifetime of TCs in La Niña is longer than El Niño years. The mean number of TC days per year is significantly higher in La Niña (7.64 days) than El Niño (3.68 days) years (statistically significant at 95% confidence level). The longer (short) life is also a plausible cause for higher (less) intensification of the TCs in La Niña (El Niño) years over BoB. The mean number of landfalling TCs during El Niño and La Niña is 0.41 and 0.68 per year, respectively. About 83% of the total landfalling TCs move westward and make landfall at south of 17°N over eastern coast of India during El Niño years. Conversely, in La Niña years, about 73% of the total landfalling TCs curved towards northwest and northward and make landfall at north of 17°N over eastern coast of India, Bangladesh and Myanmar. Apart from this, the TCs also exhibits a large spatial variation during different above and below normal ENSO phases (Figure 4c–f). The mean genesis location during El Niño (AN) and El Niño (BN) is 88°10'E, 8°85'N and 86°63'E, 10°30'N, whereas during La Niña (AN) and La Niña (BN) it is 89°38'E, 10°36'N, and 90°75'E, 10°10'N, respectively.

Therefore, in the next section an attempt has been made to examine the alterations occurred in spatial pattern of large scale environmental conditions affecting the TCs during different ENSO phases. In addition, the composites for the above normal and below normal TCs frequencies periods have also been prepared separately. The period of above normal and below normal TCs frequencies is referred as El Niño (AN) and El Niño (BN), respectively, for El Niño years, while La Niña (AN) and La Niña (BN) for La Niña years.

TABLE 3 Relationship between the TCs and Nino 3.4 anomalies during the post-monsoon season during 1972–2015

	El Niño years (15)	La Niña years (14)	Neutral years (15)
Above Normal (15)	(3) 1977, 1987, 2002	(5) 1973, 1984, 1988, 2000, 2008	(7) 1978, 1981, 1985, 1992, 1996, 2005, 2013
Normal (11)	(2) 1982, 2014	(7) 1975, 1983, 1995, 1998, 1999, 2010, 2011	(2) 1980, 2012
Below Normal (18)	(10) 1972, 1976, 1986, 1991, 1994, 1997, 2004, 2006, 2009, 2015	(2) 1974, 2007	(6) 1979, 1989, 1990, 1993, 2001, 2003

Note: Figures within the parentheses are the number of years.

**FIGURE 4** Genesis location (dots) and tracks (lines) of TCs under different (a) El Niño, (b) La Niña, (c) El Niño (AN), (d) La Niña (AN), (e) El Niño (BN) and (f) La Niña (BN) years during post-monsoon season over BoB (1972–2015)

3.3 | Impact of ENSO on BoB environmental conditions during peak TCs season

The environmental conditions of BoB that affects the TCs characteristics, are considerably modulated by ENSO (Camargo *et al.*, 2007; Felton *et al.*, 2013). The key environmental parameters such as OLR, RH, SSTAs, low-level wind flow, geopotential height and VWS affect the formation of TCs over BoB (Singh *et al.*, 2001; Pattanaik, 2005; Pattanaik and Rama Rao, 2009; Kikuchi and Wang, 2010; Yanase *et al.*, 2012). Therefore, in this section, ENSO induced alterations in large scale environmental parameters have been examined for the period 1972–2015. The composites of parameters have been prepared for the years when the frequency of TCs is above normal and below normal during different El Niño and La Niña years (Table 3).

3.3.1 | Outgoing OLR

OLR anomalies are inversely proportional to the convective activity over a region. Figure 5 exhibits the pattern of OLR anomalies under different El Niño and La Niña regimes. It has been witnessed that ENSO significantly modulates the OLR anomaly pattern over the BoB. During El Niño conditions, OLR anomalies are positive (less convective activity) over eastern BoB, Andaman Sea and Gulf of Thailand (Figure 5a). The convective activity over this region is a result of heat and moisture supply from high SSTs and the rising branch of the Walker circulation. However, the rising branch of Walker circulation and associated convective activities shift eastward as a result of higher SSTs over central Pacific during El Niño conditions. Negative anomalies are found only over western and southwestern parts of BoB. The higher convective activity over western and south-

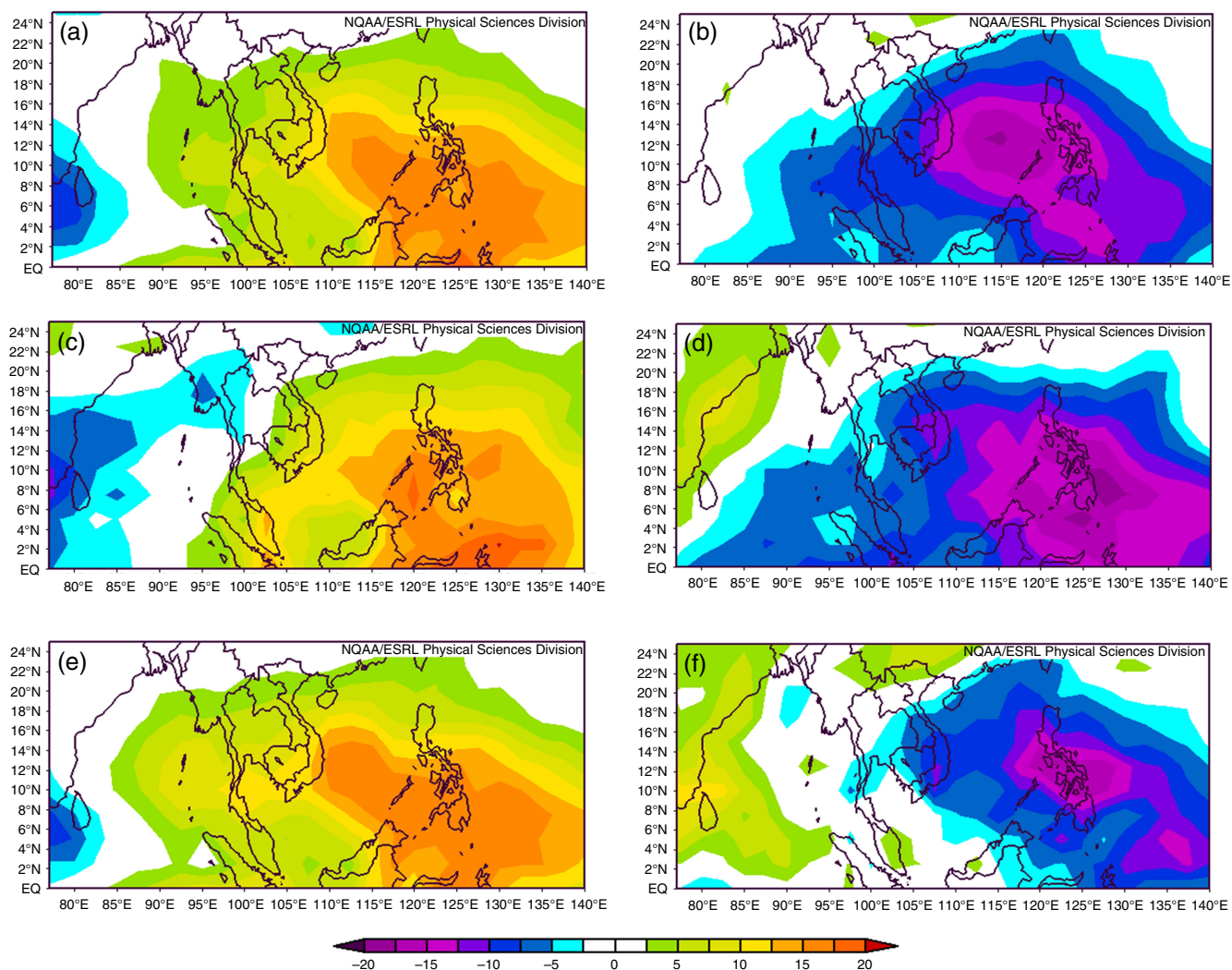


FIGURE 5 Composites of OLR anomalies at 500 hPa during post-monsoon season under different (a) El Niño, (b) La Niña, (c) El Niño (AN), (d) La Niña (AN), (e) El Niño (BN) and (f) La Niña (BN) conditions over BoB [Colour figure can be viewed at wileyonlinelibrary.com]

western parts over BoB leads to westward shift in TCs genesis during El Niño years. Conversely, a contrasting pattern is noticed in the occurrence of convective activities during La Niña years. Figure 5b exhibits the negative OLR anomalies (more convective activity) over eastern BoB (east of 90°E) and western Pacific. The higher convective activity over this region causes eastward shift in TCs genesis in La Niña years over BoB. The rising branch of the Walker circulation over western Pacific and Indonesian region creates favourable environmental conditions for convective activity and formation of TCs over BoB during La Niña years. Various other studies have also exhibited the impact of anomalous Walker circulation on TC activity for different basins (Chan, 1985; Chen *et al.*, 1998; Wang and Chan, 2002).

The composite plots of OLR anomalies for above normal and below normal TCs frequency periods also exhibit an interesting pattern. During El Niño (AN), the region of enhanced convective activity (negative OLR anomalies) of Arabian Sea is extended over BoB, while less convective activity (positive OLR anomalies) persists over large portion of BoB during El Niño (BN) (Figure 5c,e). During La Niña (AN), the region of positive OLR anomalies is positioned only along the eastern coast of India; however, southern and southeastern BoB has experienced strong convective activity (negative OLR anomalies) (Figure 5d). The region of positive OLR anomalies (less convection) is spread over a large portion of BoB during La Niña (BN) conditions (Figure 5f). Normally, in La Niña conditions, region of high convective activity is found over western Pacific and BoB upto 90°E. However, in La Niña (BN) conditions, this region of high convective activity is relatively small and extends up to 110°E with a northward shift from Indonesian and western Pacific region. Hence, less number of TCs over BoB during La Niña (BN) period can be ascribed to northward shift of this convective region in the western Pacific Ocean, which is in tune with earlier studies (Pattanaik and Rajeevan, 2007).

3.3.2 | Relative humidity

Dry mid troposphere is unfavourable for the initiation and persistence of widespread convective activity. Sufficient mid-tropospheric RH (a minimum threshold of 40%) is necessary for cyclogenesis (Gray, 1968, 1975). Figure 6 exhibits the 500 hPa RH anomalies under different El Niño and La Niña conditions. The anomalies over BoB are negative for El Niño years which are unfavourable for cyclogenesis and positive for La Niña years favouring the cyclogenesis (Figure 6a,b). High RH leads to the releasing of latent heat that is essential for TCs formation and intensification. High moisture transport to the mid-tropospheric

level can be attributed to the rising limb of Walker circulation during La Niña years over this region.

Frequency of TCs is above normal when RH anomalies are slightly higher over BoB during El Niño (AN) (Figure 6c), however, strong negative RH anomalies have been witnessed over entire BoB in El Niño (BN) period (Figure 6e). During La Niña (AN), negative RH anomalies are found only over small region of eastern coast of India, whereas anomalies have a positive spread from western Pacific to eastern BoB up to 87°E (Figure 6d). Conversely, negative anomalies are extended from Arabian sea to western BoB up to 87°E during La Niña (BN) years (positive anomalies found only over northeast BoB) (Figure 6f).

3.3.3 | Sea surface temperature (SST)

SST plays a crucial role in controlling the genesis and intensity of TCs (Kotal *et al.*, 2009; Yu and McPhaden, 2011; Sebastian and Behera, 2015). Figure 7a,b represents the SST conditions over BoB during ENSO. It is evident that SSTAs are positive in El Niño over entire BoB, while negative anomalies have been witnessed in La Niña years. However, the magnitude of SSTAs does not exhibit the significant difference. Earlier, Girishkumar and Ravichandran (2012) have found that SST is a little higher during El Niño ($>0.25^{\circ}\text{C}$) than La Niña years over BoB. The mean SST is higher ($>28^{\circ}\text{C}$) than the threshold value of SST (26.5°C) for cyclogenesis in both El Niño and La Niña conditions (Gray, 1975). The cooling of SST is attributed to the evaporation caused by unusual strong winds force in La Niña, whereas weaker winds permit for SST to rise in the southern BoB during El Niño years (Felton *et al.*, 2013). In addition, reduced (enhanced) convective activity during El Niño (La Niña) allows (blocks) solar radiations to reach the ocean surface, causing warming (cooling) of BoB.

The composites of SSTAs during above and below normal El Niño years have been demonstrated in Figure 7c,e. It has been observed that SSTAs are high (low) in the above normal TCs years (below normal TCs years) under El Niño conditions. Hence, higher SST, OLR and mid-tropospheric level humidity allows TCs to form in El Niño (AN) years over BoB. In La Niña (AN) years SSTAs are normal, whereas strong negative SSTAs have been witnessed during below normal years (La Niña) particularly over southwestern BoB (Figure 7d,f). Although SST is greater than 28°C during La Niña (BN) (figure not shown), however, only high SST is not enough to cause cyclogenesis.

3.3.4 | Low-level winds (850 hPa)

Several studies have found out that the low-level wind flow (850 hPa) significantly controls the formation and strengthening

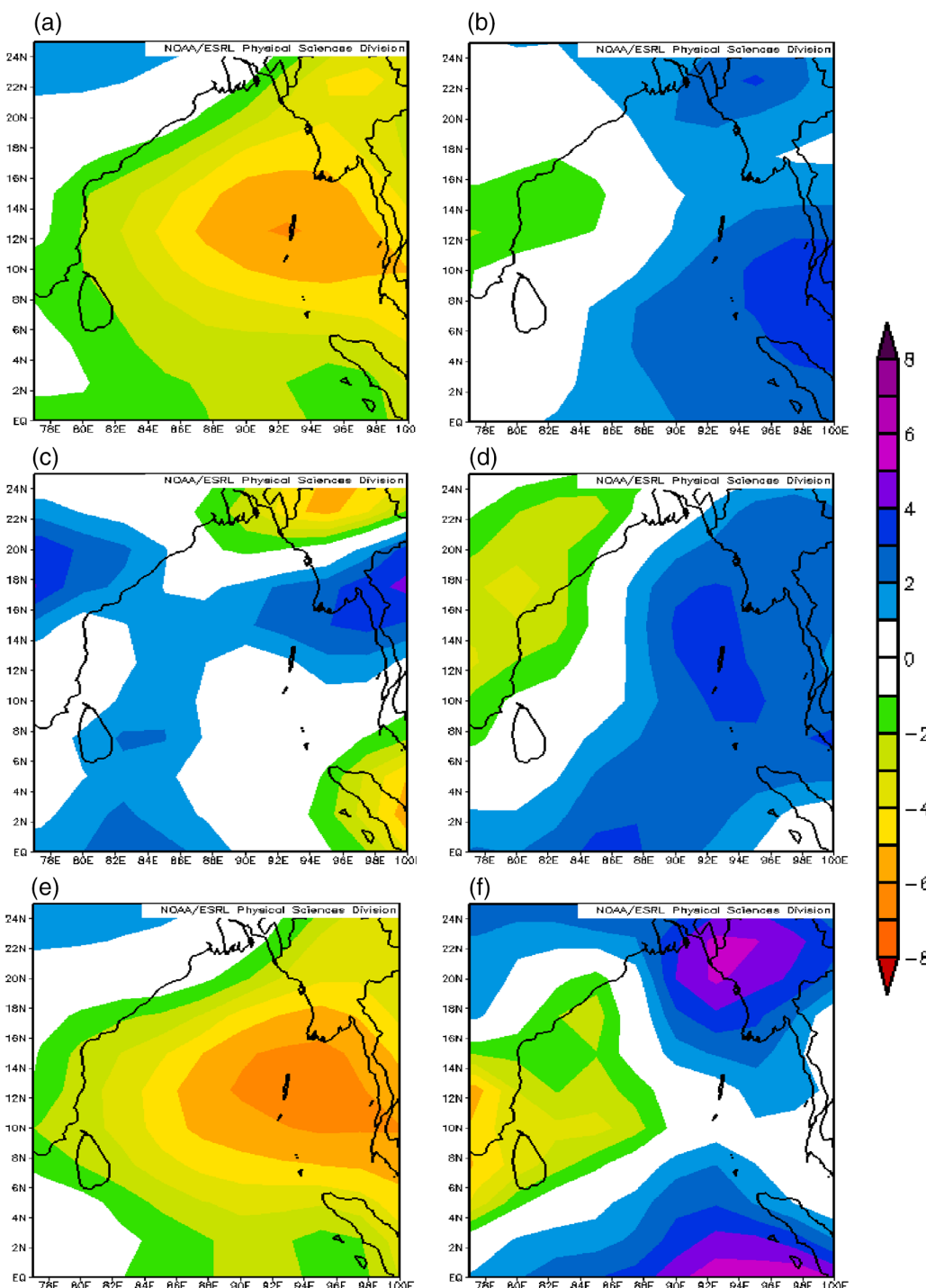


FIGURE 6 Same as Figure 5, but for 500 hPa RH anomalies [Colour figure can be viewed at wileyonlinelibrary.com]

of TCs (McBride and Zehr, 1981; Chan and Kwok, 1999; Chan, 2000; Chia and Ropelewski, 2002; Pattanaik and Rajeevan, 2007). Figure 8a,d exhibits the pattern of composite low-level winds (850 hPa) anomalies for different ENSO phases. Anomalous anticyclonic (cyclonic) circulation pattern is unfavourable (favourable) for the genesis of TCs over BoB during El Niño (La Niña) years. Existence of cyclonic flow forms the low-level cyclonic vorticity during La Niña years,

while anticyclonic flow generates the anticyclonic vorticity over BoB. Simultaneously, similar circulation pattern can be seen over South China Sea in different ENSO phases. Chan (2000) has observed the anomalous anticyclonic (cyclonic) flow at lower levels (850 hPa) in the below (above) normal TC frequency years in northwest Pacific.

In El Niño (AN) years when TCs frequency is above normal, anticyclonic circulation pattern is weak and shifted

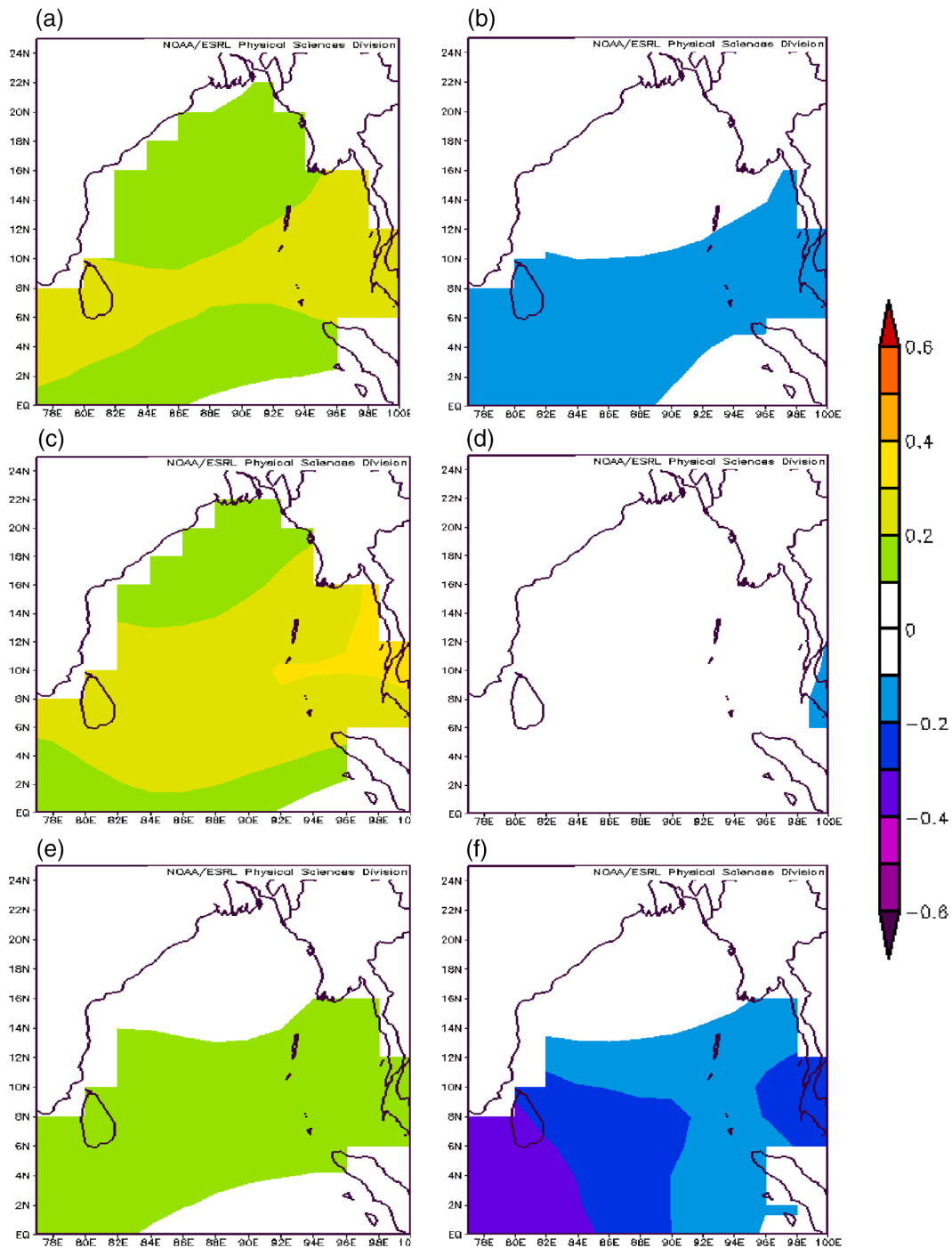


FIGURE 7 Same as Figure 5, but for SST anomalies [Colour figure can be viewed at wileyonlinelibrary.com]

towards northeast BoB, however, northeast-southwest trough line from western BoB to the southern Arabian Sea with embedded cyclonic circulation (Figure 8b). During El Niño (BN) years, a vivid anticyclonic pattern is evident over BoB (Figure 8c). Like La Niña, strong cyclonic circulation pattern can be seen in La Niña (AN) years over entire BoB and South China Sea (Figure 8e). However, this cyclonic circulation pattern shifts towards northeast BoB in La Niña (BN) years (Figure 8f).

3.3.5 | Geopotential height (500 hPa)

Geopotential height denotes the actual height of the pressure surface above mean sea level and basically indicates the position of trough and ridge in the middle troposphere (500 hPa). Negative geopotential height anomalies (low heights) indicate the trough or cyclones at mid-tropospheric level (Nath *et al.*, 2016). Composite plots of 500 hPa geopotential heights anomalies clearly indicate the distinct

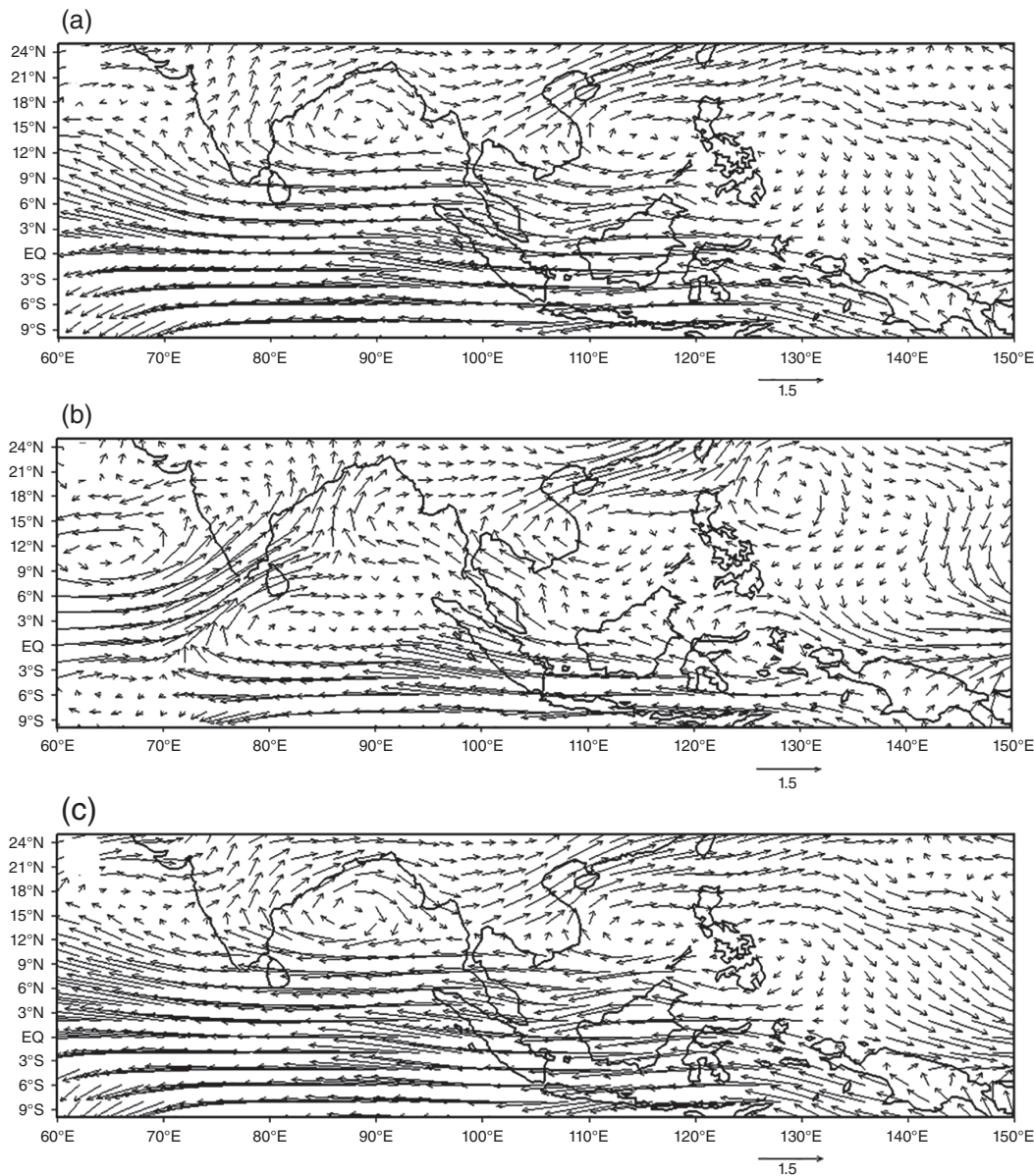


FIGURE 8 Composites of 850 hPa wind anomalies during post-monsoon season under different (a) El Niño, (b) El Niño (AN), (c) El Niño (BN), (d) La Niña, (e) La Niña (AN) and (f) La Niña (BN) conditions over BoB

large scale patterns with positive anomalies during El Niño and negative anomalies during La Niña years consistent with the below normal and above normal TCs frequency (Figure 8a,b). As discussed by Chan (1985) the sinking motion associated with the falling limb of Walker circulation over western Pacific is close to BoB, which is responsible for the anomalous high pressure and hence the positive geopotential anomalies over this region during El Niño conditions. This anomalous high pressure inhibits the TC activities during El Niño years. When the geopotential height anomalies are plotted separately for above and below normal TCs frequency years for El Niño and La Niña conditions (Figure 8c-f), the broad patterns look similar with positive and negative anomalies with no

significant difference in their magnitudes over BoB. Low height can be seen in El Niño (AN) than El Niño (BN) period. Interestingly, very low geopotential heights have been observed in La Niña (BN) years. However, low mid-level RH, less convective activity (high OLR) makes the unfavourable conditions for cyclogenesis in La Niña (BN) period.

3.3.6 | Vertical wind shear

The VWS is a large scale parameter that plays a key role in TCs genesis and its intensification. High VWS is unfavourable for the TCs genesis and development, whereas low VWS favours (Gray, 1968; DeMaria, 1996; Maloney

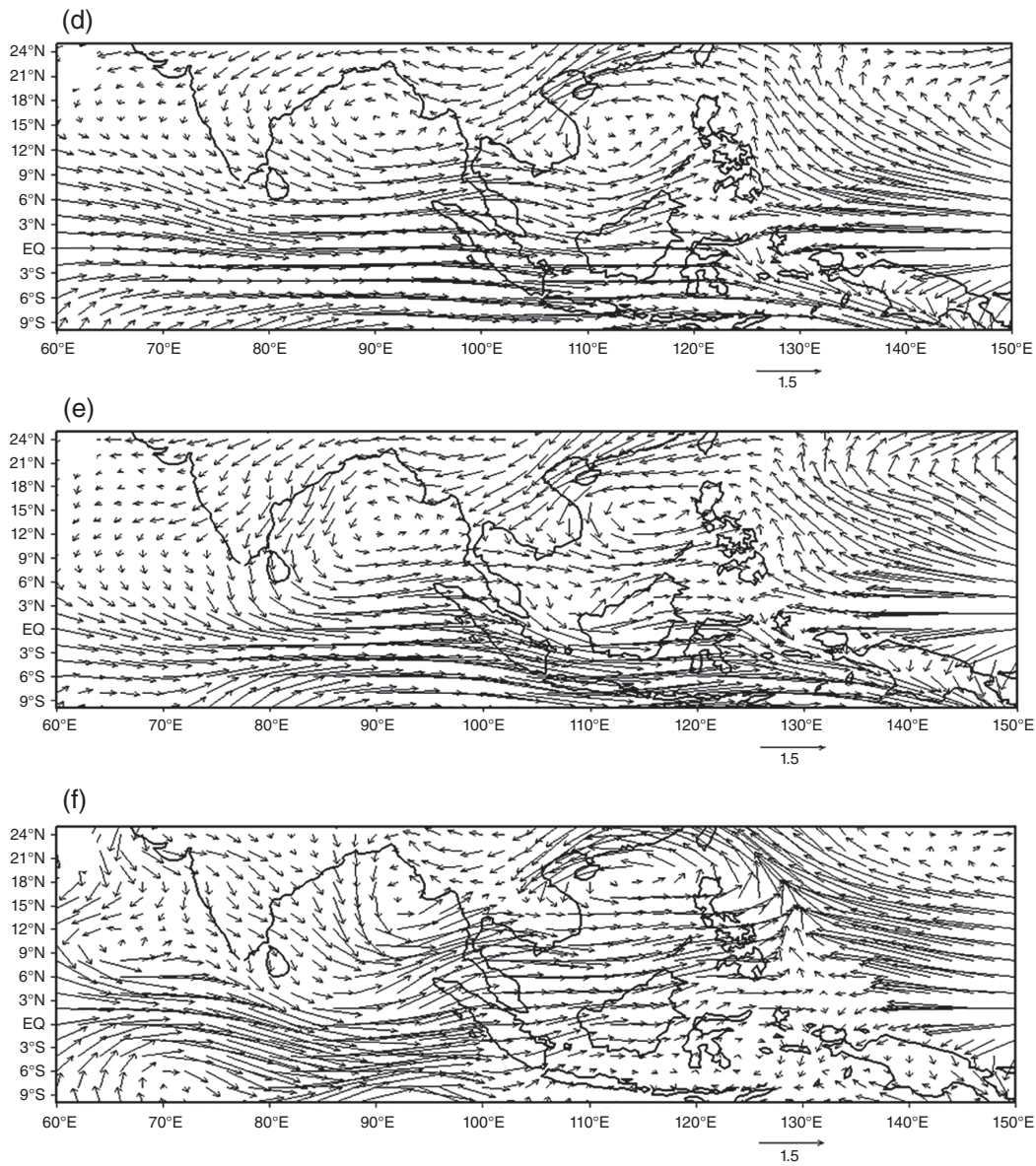


FIGURE 8 (Continued)

and Hartmann, 2000; Zehr, 2003). The VWS is relatively low (high) during La Niña (El Niño) years, which contribute to the enhanced (reduced) TC activity over BoB (Figure 9a, b). Likewise, the spatial patterns of VWS under different La Niña (El Niño) above and below normal years are almost analogous to the La Niña (El Niño) (Figure 9c–f). The zone of lowest VWS is found towards equatorial areas over the basin during both El Niño and La Niña years.

4 | SUMMARY AND CONCLUSIONS

The present study is an attempt to investigate the TC activity over BoB in relation to ENSO during post-monsoon season for the period 1972–2015. Analysis exhibits no statistical

significant increasing or decreasing trends in the frequency of TCs and both energy metrics (ACE and PDI) over BoB. However, ENSO significantly controls the TC activity over BoB. Niño 3.4 SSTAs are negatively correlated with the TC activity. Frequency and intensity of TCs is more during La Niña than El Niño years. The mean ACE, PDI and lifetime of TCs is significantly higher during La Niña than El Niño years (significant at 95% confidence level). Genesis locations of TCs have shifted towards east (west) of 89°E longitude and tend to make landfall more northward during La Niña (El Niño) years, which exhibits the more recurring nature of the tracks of TCs in La Niña than El Niño years. These variations in the TCs characteristics are attributed to ENSO forced alteration in the large scale environmental conditions over BoB.

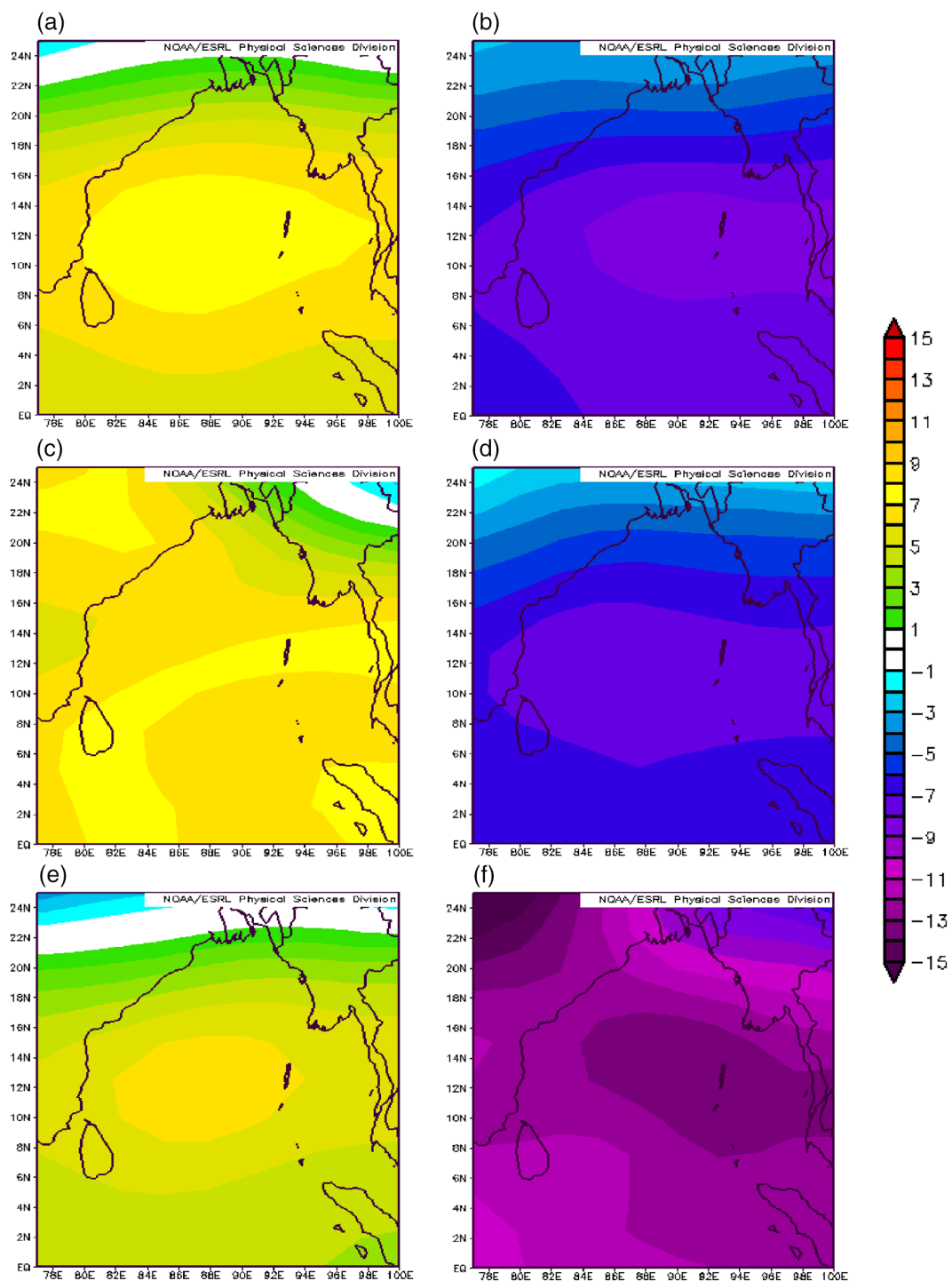


FIGURE 9 Same as Figure 5, but for 500 hPa GPH anomalies [Colour figure can be viewed at wileyonlinelibrary.com]

OLR anomalies are negative (more convective activity) over eastern and southeastern BoB, Andaman Sea and Gulf of Thailand in cold conditions (La Niña) attributed to the rising limb of the Walker circulation. However, this region of high convective activity shifts eastward in warm conditions (El Niño). Negative anomalies are found only over a small southwestern part of BoB. The higher convective activity over western and southwestern parts of BoB leads to

westward shift in TCs genesis during El Niño years. Besides, high moisture transport to the mid-tropospheric level associated with the rising limb of Walker circulation is essential for TC formation and intensification during La Niña years. Although, SST is higher than 28°C and magnitude of SSTAs does not exhibit the significant difference under different ENSO phases. However, only high SST is not sufficient for the TCs formation. Low-level winds show

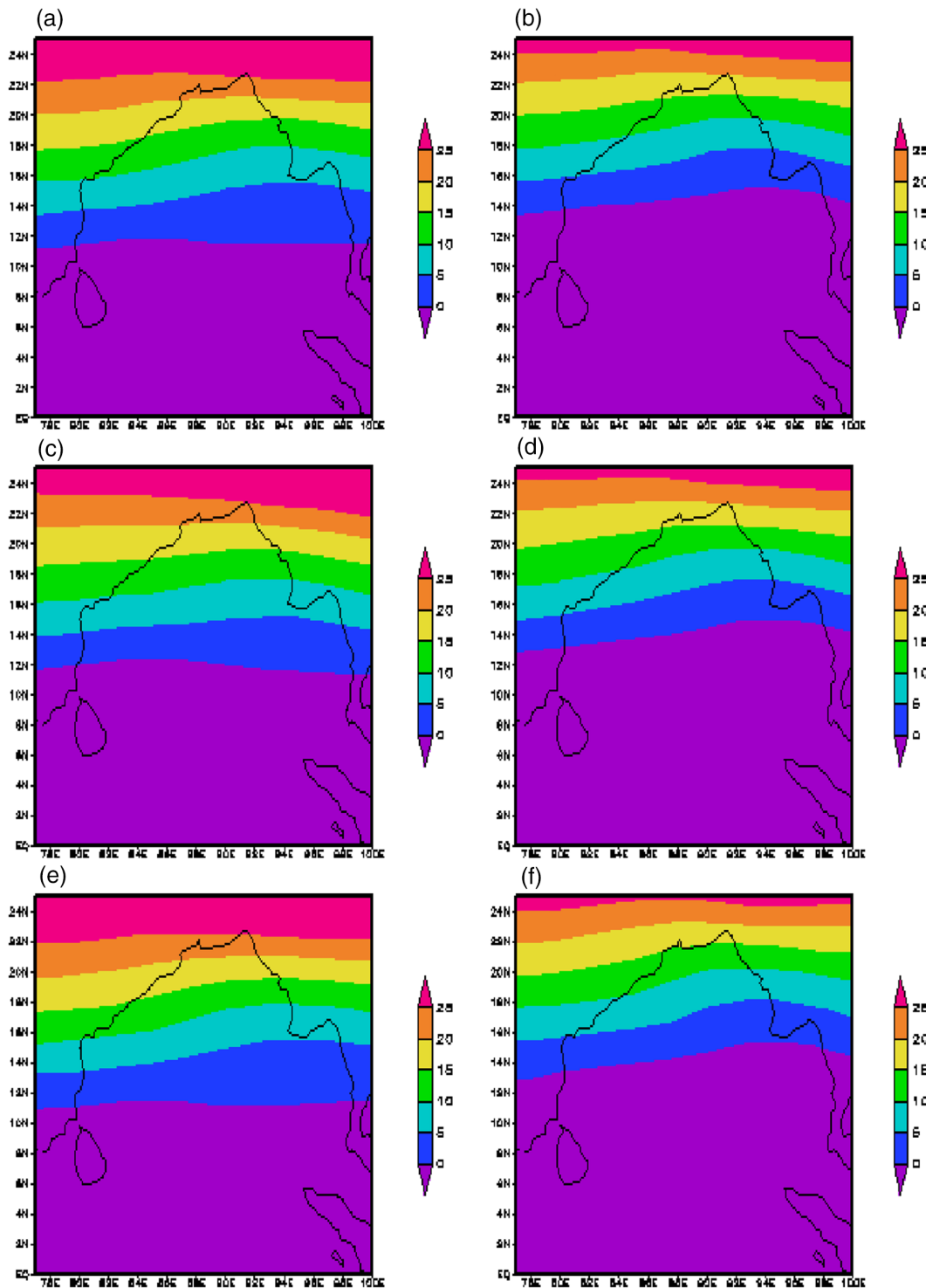


FIGURE 10 Same as Figure 5, but for mean VWS (200–850 hPa) [Colour figure can be viewed at wileyonlinelibrary.com]

the anticyclonic (cyclonic) circulation pattern, which is unfavourable (favourable) for the genesis of TCs over north BoB during El Niño (La Niña) years. Presence of cyclonic flow forms the low-level cyclonic vorticity during La Niña years, while anticyclonic flow creates the anticyclonic vorticity over BoB. Composite plots of 500 hPa geopotential heights anomalies are corresponding to the frequency of TCs

over BoB. The sinking motion associated with the falling limb of Walker circulation is responsible for the anomalous high pressure over this region which inhibits the TC activities during El Niño conditions. The VWS is relatively low (high) in cold (warm) conditions, which contribute to the enhanced (reduced) TC activity over BoB. Overall, it can be said that the large scale atmospheric and oceanic conditions

are favourable for the genesis and strengthening of TCs in La Niña than El Niño years.

In addition, TCs frequency is above normal in El Niño (AN) years owing to relatively high convective activity and RH, cyclonic circulation pattern, low geopotential heights and low VWS in spite of prevalence of warm conditions whereas these conditions are reverse in El Niño (BN) years. Similarly, above normal TCs frequency is a result of high convective activity, more RH, high SST and cyclonic circulation pattern during La Niña (AN), whereas these conditions are reverse in La Niña (BN) years in spite of cold conditions over BoB.

ACKNOWLEDGEMENTS

The authors sincerely thank the anonymous reviewers for critical comments and constructive suggestions, which improved the overall quality of the manuscript.

ORCID

Omvir Singh  <https://orcid.org/0000-0003-3594-4215>

REFERENCES

- Anandh, T.S., Das, B.K., Kumar, B., Kuttippurath, J. and Chakraborty, A. (2018) Analyses of the oceanic heat content during 1980–2014 and satellite-era cyclones over bay of Bengal. *International Journal of Climatology*, 38, 5619–5632.
- Balaguru, K., Leung, L.R., Lu, J. and Foltz, G.R. (2016) A meridional dipole in premonsoon Bay of Bengal tropical cyclone activity induced by ENSO. *Journal of Geophysical Research-Atmospheres*, 121, 6954–6968.
- Bell, G.D., Halpert, M.S., Schnell, R.C., Higgins, R.W., Lawrimore, J., Kousky, V.E., Tinker, R., Thiaw, W., Chelliah, M. and Artusa, A. (2000) Climate assessment for 1999. *Bulletin of the American Meteorological Society*, 81, 1328.
- Biswas, H.R. and Kundu, P.K. (2018) A principal component analysis based model to predict post-monsoon tropical cyclone activity in the Bay of Bengal using oceanic Niño index and dipole mode index. *International Journal of Climatology*, 38, 2415–2422.
- Bjerknes, J. (1969) Atmospheric teleconnections from the equatorial Pacific. *Monthly Weather Review*, 97, 163–172.
- Camargo, S.J., Emanuel, K.A. and Sobel, A.H. (2007) Use of a genesis potential index to diagnose ENSO effects on tropical cyclone genesis. *Journal of Climate*, 20, 4819–4834.
- Camargo, S.J., Robertson, A.W., Barnston, A.G. and Ghil, M. (2008) Clustering of eastern North Pacific tropical cyclone tracks: ENSO and MJO effects. *Geochemistry, Geophysics and Geosystems*, 9(6), Q06V05.
- Camargo, S.J. and Sobel, A.H. (2005) Western North Pacific tropical cyclone intensity and ENSO. *Journal of Climate*, 18, 2996–3006.
- Chan, J.C.L. (1985) Tropical cyclone activity in the northwest Pacific in relation to the El Niño/Southern Oscillation phenomenon. *Monthly Weather Review*, 113, 599–606.
- Chan, J.C.L. (2000) Tropical cyclone activity in the western North Pacific associated with El Niño and La Niña events. *Journal of Climate*, 13, 2960–2972.
- Chan, J.C.L. and Kwok, R.H.F. (1999) Tropical cyclone genesis in a global NWP model. *Monthly Weather Review*, 127, 611–624.
- Chang, P., Yamagata, T., Schopf, P., Behera, S.K., Carton, J., Kessler, W.S., Meyers, G., Qu, T., Schott, F., Shetye, S. and Xie, S.-P. (2006) Climate fluctuations of tropical coupled systems—the role of ocean dynamics. *Journal of Climate*, 19, 5122–5174.
- Chen, G. and Huang, R. (2006) The effect of warm pool thermal states on tropical cyclone in West Northwest Pacific. *Journal of Tropical Meteorology*, 22, 527–532.
- Chen, T.C., Wang, S.Y. and Yen, M.C. (2006) Interannual variation of tropical cyclone activity over the western North Pacific. *Journal of Climate*, 19, 5709–5720.
- Chen, T.C., Weng, S.P., Yamazaki, N. and Kiehne, S. (1998) Interannual variation in the tropical cyclone formation over the Western North Pacific. *Monthly Weather Review*, 126, 1080–1090.
- Chia, H.H. and Ropelewski, C.F. (2002) The interannual variability in the genesis location of tropical cyclones in the northwest Pacific. *Journal of Climate*, 15, 2934–2944.
- Chittibabu, P.S., Dube, K., Macnabb, J.B., Murty, T.S., Rao, A.D., Mohanty, U.C. and Sinha, P.C. (2004) Mitigation of flooding and cyclone hazard in Orissa, India. *Natural Hazards*, 31, 455–485.
- Chu, J.H., Sampson, C.R., Levine, A.S., Fukada E. (2002). *The Joint Typhoon Warning Center tropical cyclone best-tracks, 1945–2000*. U.S. Naval Research Laboratory Report (pp. 22), NRL/MR/7540-02-16.
- Chu, P.S. and Wang, J. (1997) Tropical cyclone occurrences in the vicinity of Hawaii: are the differences between El Niño years significant? *Journal of Climate*, 10, 2683–2689.
- Clark, J.D. and Chu, P. (2002) Interannual variation of tropical cyclone activity over the central North Pacific. *Journal of the Meteorological Society of Japan*, 80, 403–418.
- DeMaria, M. (1996) The effect of vertical shear on tropical cyclone intensity change. *Journal of the Atmospheric Sciences*, 53, 2076–2087.
- Dube, S.K., Rao, A.D., Sinha, P.C., Murty, T.S. and Bahuleyan, N. (1997) Storm surge in bay of Bengal and Arabian Sea: the problem and its prediction. *Mausam*, 48, 288–304.
- Emanuel, K.A. (2005) Increasing destructiveness of tropical cyclones over the past 30 years. *Nature*, 436, 686–688.
- Felton, C.S., Subrahmanyam, B. and Murty, V.S.N. (2013) ENSO-modulated cyclogenesis over the Bay of Bengal. *Journal of Climate*, 26, 9806–9818.
- Fritz, H.M., Blount, C.D., Thwin, S., Thu, M.K. and Chan, N. (2009) Cyclone Nargis storm surge in Myanmar. *Nature Geoscience*, 2, 448–449.
- Girishkumar, M.S. and Ravichandran, M. (2012) The influences of ENSO on tropical cyclone activity in the Bay of Bengal during October–December. *Journal of Geophysical Research*, 117(2), c02033.
- Girishkumar, M.S., Suprit, K., Vishnu, S., Thanga Prakash, V.P. and Ravichandran, M. (2015) The role of ENSO and MJO on rapid intensification of tropical cyclones in the Bay of Bengal during October–December. *Theoretical and Applied Climatology*, 120, 797–810.
- Gray, W.M. (1968) Global view of the origin of tropical disturbances and storms. *Monthly Weather Review*, 96, 669–700.

- Gray, W.M. (1975). *Tropical cyclone genesis*. Department of Atmospheric Science. Paper No. 234. Colorado: Colorado State University, Fort Collins.
- Gray, W.M. (1984) Atlantic seasonal hurricane frequency. Part I: El Niño and 30-mb quasi-biennial oscillation influences. *Monthly Weather Review*, 112, 1649–1688.
- Gutzler, D.S., Wood, K.M., Ritchie, E.A., Douglas, A.V. and Lewis, M.D. (2013) Interannual variability of tropical cyclone activity along the Pacific coast of North America. *Atmosfera*, 26, 149–162.
- Huang, B., Thorne, P., Smith, T., Liu, W., Lawrimore, J., Banzon, V., Zhang, H.M., Peterson, T.C. and Menne, M. (2015) Further exploring and quantifying uncertainties for extended reconstructed sea surface temperature (ERSST) version 4 (v4). *Journal of Climate*, 29, 3119–3142.
- Kalnay, E., Kanamitsu, M., Kistler, R., Collins, W., Deaven, D., Gandin, L., Iredell, M., Saha, S., White, G., Woollen, J., Zhu, Y., Chelliah, M., Ebisuzaki, W., Higgins, W., Janowiak, J., Mo, K.C., Ropelewski, C., Wang, J., Leetmaa, A., Reynolds, R., Jenne, R. and Joseph, D. (1996) The NCEP/NCAR 40-year reanalysis project. *Bulletin of the American Meteorological Society*, 77, 437–471.
- Kikuchi, K. and Wang, B. (2010) Formation of tropical cyclones in the northern Indian Ocean associated with two types of tropical intra-seasonal oscillation modes. *Journal of the Meteorological Society of Japan*, 88, 475–496.
- Klotzbach, P.J. (2011) El Niño-Southern Oscillation's impact on Atlantic basin hurricanes and US landfalls. *Journal of Climate*, 24, 1252–1263.
- Klotzbach, P.J. (2012) El Niño-Southern Oscillation, the Madden-Julian Oscillation and Atlantic basin tropical cyclone rapid intensification. *Journal of Geophysical Research*, 117(D14), D14104.
- Klotzbach, P.J. and Oliver, E.C.J. (2015) Variations in global tropical cyclone activity and the Madden-Julian Oscillation since the midtwentieth century. *Geophysical Research Letters*, 42, 4199–4207.
- Kotal, S.D., Kundu, P.K. and Roy Bhownik, S.K. (2009) An analysis of sea surface temperature and maximum potential intensity of tropical cyclones over the Bay of Bengal between 1981 and 2000. *Meteorological Applications*, 16, 169–177.
- Kuleshov, Y., Qi, L., Fawcett, R. and Jones, D. (2008) On tropical cyclone activity in the Southern Hemisphere: trends and the ENSO connection. *Geophysical Research Letters*, 35, 2008.
- Lander, M.A. (1994) An exploratory analysis of the relationship between tropical storm formation in the western North Pacific and ENSO. *Monthly Weather Review*, 122, 636–651.
- Li, Z., Yu, W., Li, T., Murty, V.S.N. and Tangang, F. (2013) Bimodal character of cyclone climatology in the Bay of Bengal modulated by monsoon seasonal cycle. *Journal of Climate*, 26, 1033–1046.
- Liebmann, B. and Smith, C. (1996) Description of a complete (interpolated) outgoing longwave radiation dataset. *Bulletin of the American Meteorological Society*, 77, 1275–1277.
- Mahala, B.K., Nayak, B.K. and Mohanty, P.K. (2015) Impacts of ENSO and IOD on tropical cyclone activity in the Bay of Bengal. *Natural Hazards*, 75, 1105–1125.
- Maloney, E.D. and Hartmann, D.L. (2000) Modulation of eastern North Pacific hurricanes by the Madden-Julian oscillation. *Journal of Climate*, 13, 1451–1460.
- McBride, J. and Zehr, R. (1981) Observational analysis of tropical cyclone formation. Part II: comparison of non-developing versus developing systems. *Journal of the Atmospheric Sciences*, 38, 1132–1151.
- McPhaden, M.J. (2002) El Niño and La Niña: Causes and global consequences. In: Munn, T. (Ed.) *Encyclopedia of Global Environmental Change*. Chichester: John Wiley, pp. 353–370.
- Mohapatra, M. and Kumar, V.V. (2016) Interannual variation of tropical cyclone energy metrics over North Indian Ocean. *Climate Dynamics*, 48, 1431–1445.
- Nath, S., Kotal, S.D. and Kundu, P.K. (2016) Decadal variation of ocean heat content and tropical cyclone activity over the Bay of Bengal. *Journal of Earth System Science*, 125, 65–74.
- Neumann, C.J. (1993) *Global Overview. Global guide to tropical cyclone forecasting*, Vol. 1. Geneva: World Meteorological Organization, pp. 1–1.56.
- Ng, E.K.W. and Chan, J.C.L. (2012) Interannual variations of tropical cyclone activity over the North Indian Ocean. *International Journal of Climatology*, 32, 819–830.
- Pattanaik, D.R. (2005) Variability of oceanic and atmospheric conditions during active and inactive periods of storms over the Indian region. *International Journal of Climatology*, 25, 1523–1530.
- Pattanaik, D.R. and Rajeevan, M. (2007) North-west Pacific tropical cyclone activity and July rainfall over India. *Meteorology and Atmospheric Physics*, 95, 63–72.
- Pattanaik, D.R. and Rama Rao, Y.V. (2009) Track prediction of very severe cyclone "Nargis" using high resolution weather research forecasting (WRF) model. *Journal of Earth System Science*, 118, 309–329. <https://doi.org/10.1007/s12040-009-0031-8>.
- Peduzzi, P., Chatenoux, B., Dao, H., Bono, A.D., Herold, C., Kossin, J., Mouton, F. and Nordbeck, O. (2012) Global trends in tropical cyclone risk. *Nature Climate Change*, 2, 289–294.
- Picaut, J., Ioualalen, M., Delcroix, T., Masia, F., Murtugudde, R. and Vialard, J. (2001) The oceanic zone of convergence on the eastern edge of the Pacific warm pool: a synthesis of results and implications for El Niño-Southern Oscillation and biogeochemical phenomena. *Journal of Geophysical Research*, 106(C2), 2363–2386.
- Rasmusson, E.M. and Carpenter, T.H. (1982) Variations in tropical sea surface temperature and surface wind fields associated with the Southern Oscillation/El Niño. *Monthly Weather Review*, 110, 354–384.
- Sebastian, M. and Behera, M.R. (2015) Impact of SST on tropical cyclones in North Indian Ocean. *Procedia Engineering*, 116, 1072–1077.
- Singh, O.P. (2010) Recent trends in tropical cyclone activity in the North Indian Ocean. In: Charabi, Y. (Ed.) *Indian Ocean Tropical Cyclones and Climate Change*. Dordrecht: Springer, pp. 51–54.
- Singh, O.P., Khan, T.M.A. and Rahman, M.S. (2001) Probable reasons for enhanced cyclogenesis in the Bay of Bengal during July–August of ENSO years. *Global and Planetary Change*, 29, 135–147.
- Smith, T.M. and Reynolds, R.W. (2003) Extended reconstruction of global sea surface temperature based on COADS data (1854–1997). *Journal of Climate*, 16, 1495–1510.
- Tang, B.H. and Neelin, J.D. (2004) ENSO influence on Atlantic hurricanes via tropospheric warming. *Geophysical Research Letters*, 31, L24204.
- Trenberth, K.E. (1984) Signal versus noise in the Southern Oscillation. *Monthly Weather Review*, 112, 326–332.
- Trenberth, K.E. (1997) The definition of El Niño. *Bulletin of the American Meteorological Society*, 78, 2771–2777.
- Tziperman, E.L., Cane, M.A., Zebiak, S., Xue, Y. and Blumenthal, B. (1998) Locking of El Niño's peak time to the end of the calendar

- year in the delayed oscillator picture of ENSO. *Journal of Climate*, 11, 2191–2199.
- Wang, B. and Chan, J.C.L. (2002) How strong ENSO events affect tropical storm activity over the western North Pacific. *Journal of Climate*, 15, 1643–1658.
- Wang, B. and Zhou, X. (2008) Climate variation and prediction of rapid intensification in tropical cyclones in the western North Pacific. *Meteorology and Atmospheric Physics*, 99, 1–16.
- Xu, S. and Huang, F. (2015) Impacts of the two types of El Niño on Pacific tropical cyclone activity. *Journal of Ocean University of China*, 14, 191–198.
- Yanase, W., Satoh, M., Taniguchi, H. and Fujinami, H. (2012) Seasonal and intraseasonal modulation of tropical cyclogenesis environment over the Bay of Bengal during the extended summer monsoon. *Journal of Climate*, 25, 2914–2930.
- Yu, L. and McPhaden, M.J. (2011) Ocean preconditioning of Cyclone Nargis in the Bay of Bengal: interaction between Rossby waves, surface fresh waters, and sea surface temperatures. *Journal of Physical Oceanography*, 41, 1741–1755.
- Zehr, R.M. (2003) Environmental vertical wind shear with Hurricane Bertha (1996). *Weather and Forecasting*, 18, 345–356.
- Zhao, H. and Raga, G.B. (2015) On the distinct interannual variability of tropical cyclone activity over the eastern North Pacific. *Atmosfera*, 28, 161–178.

How to cite this article: Bhardwaj P, Pattanaik DR, Singh O. Tropical cyclone activity over Bay of Bengal in relation to El Niño-Southern Oscillation. *Int J Climatol*. 2019;1–18. <https://doi.org/10.1002/joc.6165>